

Times, environments and channels of bulge formation in a Λ CDM cosmology

Gabriella De Lucia^{1*}, Fabio Fontanot¹, David Wilman², Pierluigi Monaco^{3,1}

¹*INAF - Astronomical Observatory of Trieste, via G.B. Tiepolo 11, I-34143 Trieste, Italy*

²*Max-Planck-Institut für Extraterrestrische Physik, Giessenbachstraße, D-85748 Garching, Germany*

³*Dipartimento di Astronomia, Università di Trieste, via G.B. Tiepolo 11, I-34131 Trieste, Italy*

10 November 2018

ABSTRACT

We analyze predictions from two independently developed galaxy formation models to study the mechanisms, environments, and characteristic times of bulge formation in a Λ CDM cosmogony. For each model, we test different prescriptions for bulge formation in order to quantify the relative importance of different channels. Our results show that the strong correlation between galaxy and halo mass for central galaxies, and the richer merger history of more massive systems naturally give rise to a strong correlation between galaxy mass and morphology, and between halo mass and morphological type of central galaxies. Large fractions of the bulge mass are acquired through major and minor mergers, but disc instability plays an important role, particularly for intermediate mass galaxies. We find that the modelling of disc instability events, as well as of the galaxy merger times, can affect significantly the timing of bulge formation, and the relative importance of different channels. Bulge dominated galaxies acquire their morphology through major mergers, but this can be modified by cooling of gas from the surrounding hot halo. We find that disc regrowth is a non negligible component of the evolution of bulge dominated galaxies, particularly for low to intermediate masses, and at high redshifts.

Key words: galaxies: formation – galaxies: evolution – galaxies: bulges – galaxies: interactions – galaxies: structure.

1 INTRODUCTION

Perhaps the clearest and most convenient definition of a *bulge* is that of a centrally concentrated stellar distribution, with a smooth and spherical appearance. Indeed, such a definition underlies the classification scheme introduced by Hubble (1926). In the local Universe, about 60 per cent of the total stellar mass of massive galaxies is contained in ellipticals and bulges (Gadotti 2009). It is clear then, that understanding how bulges form and evolve is integral to the question of understanding galaxy formation and evolution.

Until the early 1980s, bulges were thought to belong to the same family as elliptical galaxies, and to have formed through the same physical process(es). Several lines of evidence, however, indicated later that the class ‘bulges’ represents a heterogeneous family including systems with very different properties, and likely very different formation and evolutionary histories. Indeed, significant differences were found between the kinematics of ellipticals and bulges (e.g. Dressler & Sandage 1983; Davies & Illingworth 1983, and

references therein). It was also noted that many bulges exhibit a ‘boxy’ or ‘peanut’ shaped structure at small radii. This shape, that is unlikely to be due to the gravitational influence of the disc, was found to be associated with differential cylindrical rotation (Kormendy & Illingworth 1982). In the past decades, substantial evidence has accumulated that many bulges have ‘disc-like’ exponential profiles (e.g. Andredakis & Sanders 1994; Carollo et al. 2001; Balcells et al. 2003; Fisher & Drory 2008) and, in some cases, ‘disc-like’ cold kinematics (Kormendy 1993; Pinkney et al. 2003; Kormendy & Kennicutt 2004, and references therein). These systems are now often referred to as ‘pseudo-bulges’, as opposed to ‘classical bulges’ that are relatively featureless both dynamically and photometrically, and appear to have a close affinity with elliptical galaxies.

The current view is that classical bulges are formed through rapid collapse or hierarchical mergers of smaller objects, and corresponding dissipative gas processes. Early numerical simulations showed that close interactions can lead to a strong internal dynamical response, driving the formation of spiral arms and, in some cases, of strong bar modes. The axisymmetry of these structures induces a compression

* Email: delucia@oats.inaf.it

of the gas that can fuel nuclear starbursts and/or nuclear AGN activity (see e.g. Mihos 2004, and references therein). Simulations have also shown that the merger of two spiral galaxies of comparable mass can produce a remnant with structural and photometric properties resembling those of elliptical galaxies (e.g. Toomre & Toomre 1972; Mihos 2004; Springel, Di Matteo & Hernquist 2005). On the other hand, pseudo-bulges are thought to originate from the evolution of disc instabilities such as bars. Early simulations by Hohl (1971) showed that bar formation is accompanied by a rearrangement of disc material, which results in the formation of a high-density central core. Later and more detailed simulations have confirmed that gravitational instabilities such as spirals and bars are able to build ‘bulge-like’ structures, either through vertical resonances or through bending (‘buckling’) of the bars (e.g. Combes et al. 1990; Raha et al. 1991; Debattista et al. 2006).

All these processes are at play in the general framework of hierarchical galaxy formation: galaxies are supposed to form through the condensation of gas at the centre of dark matter haloes. Conservation of angular momentum leads to the formation of a rotationally supported disc. If the cooling is ‘rapid’ (at high redshift and in relatively small haloes), the short dynamical times lead to an intense star-burst activity. Mergers and instabilities form ‘bulges’, that can eventually grow a new disc, provided the system is fed by an appreciable cooling flow. In this framework then, bulge-dominated galaxies can be ‘transitory’ systems. The importance of disc regrowth and its correlation with the physical properties and/or environment of galaxies has, however, not been analyzed in detail.

Accurate studies of the structural and physical properties of bulges and ellipticals are now being carried out (e.g. Gadotti 2009, at low redshift). These studies and their extension to higher redshift, will likely provide important constraints on how the different population of bulges evolved as a function of cosmic time. It is therefore interesting to analyze in more detail predictions from recently published galaxy formation models, with particular regard to the question of what is the relative role of different physical mechanisms (e.g. mergers vs disc instability) in the formation of galaxy bulges, and their evolution as a function of redshift, environment and galaxy mass.

In this paper, we analyze predictions from two independently developed semi-analytic models of galaxy formation. While the models used in this study do not allow a fine classification into ‘bulges’, ‘pseudo-bulges’, or ‘bars’ to be made, they allow us to quantify the amount of mass that is contributed to the spheroidal components by different ‘channels’ (minor and major mergers, and disc instability), and to study when and in which environment(s) these processes take place. Using two different models and, within them, different prescriptions for the formation of bulges, we are able to analyze how the relative importance of different channels varies as a function of different specific physical assumptions. Some of these issues have been addressed using similar classes of models in previous studies (Parry, Eke & Frenk 2009; Benson & Devereux 2010), and we will comment on these results below. In this study, we focus on theoretical predictions, and defer a detailed comparison between model results and observational data to a future work.

The layout of the paper is as follows. In Section 2, we

introduce the galaxy formation models used in this study, focusing on those aspects of the models that are relevant for bulge formation. In Section 3, we discuss the basic trends predicted as a function of the galaxy stellar mass and of the parent halo virial mass. In Sections 4 and 5, we analyze the times and environments that characterize the formation of galaxy bulges through different channels. In Section 6, we study the formation history of ‘elliptical’ galaxies and address the issue of disc regrowth. Finally, we discuss our results, and give our conclusions in Section 7.

2 THE GALAXY FORMATION MODELS

In this paper, we consider predictions from two different and independently developed semi-analytic models of galaxy formation within a Λ CDM cosmogony. In particular, we use (i) the recent implementation of the Munich model by De Lucia & Blaizot (2007), with its generalization to the WMAP3 cosmology discussed in Wang et al. (2008); and (ii) the MORGANA model presented in Monaco, Fontanot & Taffoni (2007), and adapted to a WMAP3 cosmology as described in Lo Faro et al. (2009).

Comparisons between different specific predictions from these two models have been discussed in Fontanot et al. (2009) and Fontanot et al. (2010). A detailed analysis of the prescriptions adopted to model gas cooling and galaxy mergers is given in De Lucia et al. (2010). We refer to the original papers for more details on the modelling of various physical processes. In the following, we highlight the main differences between the implementations of these ingredients, focusing on those physical processes that are relevant for bulge formation. We also summarize the prescriptions proposed by Hopkins et al. (2009a), that we have implemented in the two models used in this study.

2.1 The WDL08 model

Cosmological framework: The model discussed in Wang et al. (2008, WDL08 hereafter) takes advantage of N-body simulations that follow the evolution of $N = 540^3$ particles within a comoving box of size $125 h^{-1} \text{Mpc}$ on a side. This corresponds to a particle mass of $7.78 \times 10^8 h^{-1} M_{\odot}$. In this study, we use their simulation with WMAP3 cosmological parameters: $\Omega_m = 0.226$, $\Omega_b = 0.04$, $\Omega_{\Lambda} = 0.774$, $n = 0.947$, and $\sigma_8 = 0.722$. The Hubble constant is parametrized as $H_0 = 100 h \text{ km s}^{-1} \text{Mpc}^{-1}$, and this particular simulation assumes $h = 0.743$.

Merger trees: Simulation data were stored at 64 output times, that are approximately logarithmically spaced between $z=20$ and 1, and approximately linearly spaced in time thereafter. Group catalogues were constructed using a standard friends-of-friends (FOF) algorithm, with a linking length of 0.2 in units of the mean particle separation. Each group was then decomposed into a set of disjoint substructures using the algorithm SUBFIND (Springel et al. 2001), which iteratively determines the self-bound subunits within a FOF group. The most massive of these substructures is often referred to as the *main halo*, while this and all other substructures are all referred to as *subhaloes* or *substructures*. Only subhaloes that retain at least 20 bound parti-

cles after a gravitational unbinding procedure are considered ‘genuine’ subhaloes, therefore setting the subhalo detection limit to $2.22 \times 10^{10} M_{\odot}$. These catalogues were then used to construct merger history trees of all gravitationally self-bound substructures, as explained in detail in Springel et al. (2005, see also De Lucia & Blaizot 2007).

Galaxy mergers: At variance with the other model used in this study, the WDL08 one follows dark matter haloes after they are accreted onto larger systems. This allows the dynamics of satellite galaxies residing in infalling haloes to be properly followed, until the parent dark matter substructure is ‘destroyed’ (i.e. falls below the resolution limit of the simulation) by tidal truncation and stripping (e.g. De Lucia et al. 2004; Gao et al. 2004). When this happens, galaxies are assigned a residual surviving time using the classical dynamical friction formula¹. The residual merging time is estimated from the relative orbit of the two merging objects, at the time of subhalo disruption.

In the case of a ‘minor’ merger, the stellar mass of the merged galaxy is transferred to the bulge component of the remnant galaxy, and a fraction of the combined cold gas from both galaxies is turned into stars as a result of the merger. The efficiency of the merger-driven starburst is parametrized adopting the formulation proposed by Somerville et al. (2001):

$$e_{\text{burst}} = \beta_{\text{burst}} (m_2/m_1)^{\alpha_{\text{burst}}}$$

where m_2/m_1 is the baryonic (gas + stars) mass ratio, and $\alpha_{\text{burst}} = 0.7$ and $\beta_{\text{burst}} = 0.56$ have been chosen to provide a good fit to the numerical simulations of Cox et al. (2008).

All stars that form during the burst, as well as all remaining cold gas, are added to the disc of the remnant galaxy. If the baryonic mass ratio of the merging galaxies is larger than 0.3, we assume that we witness a ‘major’ merger, that gives rise to a more significant starburst and destroys the disc of the central galaxy completely, leaving a purely spheroidal stellar remnant. The remnant galaxy can grow a new disc later on, provided it is fed by an appreciable cooling flow.

Disc instability: bulges can also grow through disc instabilities, that are assumed to take place when the following condition is verified (Efstathiou, Lake & Negroponte 1982):

$$\frac{V_{\text{disc}}}{(G m_{\text{disc}}/r_{\text{disc}})^{1/2}} \lesssim \epsilon_{\text{lim}} \quad (1)$$

In the above equation, m_{disc} , r_{disc} , and V_{disc} are the stellar mass, the radius, and the velocity of the disc, respectively. In this model, $V_{\text{disc}} = V_{\text{max}}$, and is computed directly from the underlying N -body simulation; r_{disc} is the half-mass radius of the disc that, for an exponential disc, is equal to $1.68 \times R_{\text{d}}$; R_{d} is the disc scale length, and is computed following Mo, Mao & White (1998). The model assumes $\epsilon_{\text{lim}} = 0.75$, that is chosen in order to reproduce the observed morphological mix in the local Universe. For each galaxy, and at each time-step, we check whether the instability condition is verified and, when this is the case, we transfer enough stellar mass from the disc to the bulge so as to restore stability.

¹ For a detailed discussion of the adopted formulation, and for a comparison with different implementations, see De Lucia et al. (2010).

2.2 The MORGANA model

Cosmological framework: The results from the MORGANA model presented in this study have been obtained using a $144 h^{-1} \text{Mpc}$ box with $N = 1000^3$ particles, and adopting a cosmology with $\Omega_{\text{m}} = 0.24$, $\Omega_{\Lambda} = 0.76$, $\sigma_8 = 0.8$, $n = 0.96$, and $h = 0.72$. The dark matter data used by MORGANA are obtained using the code PINOCCHIO (Monaco et al. 2002). This algorithm, based on Lagrangian perturbation theory, has been shown to provide mass assembly histories of dark matter haloes that are in excellent agreement with results from numerical simulations (Li et al. 2007).

Merger trees: For details on the construction of merger trees, we refer to Monaco et al. (2007) and Taffoni et al. (2002). We note that PINOCCHIO does not provide information on dark matter substructures, so MORGANA is essentially based on the equivalent of FOF merger trees.

Galaxy mergers: In order to model the orbital decay of dark matter subhaloes and galaxy mergers, MORGANA uses a slightly updated version of the fitting formulae provided by Taffoni et al. (2003). These take into account dynamical friction, mass loss by tidal stripping, tidal disruption of substructures, and tidal shocks. In practice, whenever two (FOF) haloes merge, the galaxy associated with the smaller halo is assigned a galaxy merger time by interpolating between the two extreme cases of a ‘live satellite’ (where the object is subject to significant mass losses) and that of a ‘rigid’ satellite (that does not suffer a significant mass loss). We refer to the original paper for details on the implementation.

As in WDL08, MORGANA distinguishes between minor and major galaxy mergers, using the same baryonic mass ratio threshold (0.3). During a minor merger, the stellar mass and the cold gas of the accreted satellite are added to the bulge component of the remnant galaxy, whose disc is unaffected by the merger. During major mergers, the stellar and gaseous disc of the remnant galaxy are destroyed and relaxed into a single spheroidal component. The cold gas associated with the bulge can be efficiently converted into stars, and this occurs on very short time-scales (effectively triggering a ‘starburst’) during major mergers. As in WDL08, the remnant galaxy can grow a new disc, out of the gas cooling at later times.

Disc instability: For this process, MORGANA adopts the same stability criterion as in the WDL08 model, but uses different definitions for the mass, radius and velocity of the disc, and assumes $\epsilon_{\text{lim}} = 0.7$ (Lo Faro et al. 2009). As for WDL08, this is chosen in order to reproduce the observed morphological mix in the local Universe. In this model, m_{disc} is the total baryonic mass of the disc, r_{disc} is the disc scale-length (also computed following Mo et al. 1998), and V_{disc} is the rotational velocity of the disc, computed as detailed in Monaco et al. (2007). When the instability condition is verified, half of the baryonic mass of the disc is transferred to the bulge component. As explained above, the presence of a significant amount of cold gas in the bulge can trigger a burst of star formation.

Additional processes: MORGANA includes additional physical mechanisms that influence the assembly history of bulges. In particular, the model allows infall of gas onto an existing bulge, by a fraction equal to the fraction of disc mass embedded in the bulge. In addition, the model takes

into account tidal stripping of stars in satellites, and assumes that a fraction ($f_{sca} = 0.7$ in the standard model) of satellite stars are unbound during major mergers and incorporated into a ‘diffuse’ light component. In the following, we will neglect the second process (i.e. we will assume $f_{sca} = 0$). We have verified, however, that this does not alter significantly any of the results discussed in this study.

2.3 Model differences

The previous sections clarify that the two models used in this study differ in a number of details. As we will see in the following, some of these are reflected in significant differences between model predictions. In this section, we briefly comment on these expectations.

In De Lucia et al. (2010), we compared the merger model adopted in MORGANA with that employed in WDL08, and showed that the former provides merger times that are systematically shorter (by an order of magnitude) than those predicted by the latter. This will likely translate into a different relative importance of the merger channel. In order to quantify the significance of this different treatment of galaxy mergers, we will also show results from MORGANA obtained using longer merger times.

Another significant difference between the two models is related to the adopted treatment of disc instability: although both models are based on the criterion proposed by Efstathiou et al. (1982), they adopt different definitions for the mass, radius and velocity of the disk, and instability events have rather different consequences. In WDL08, disc instability is evaluated only for the stellar component, and when instabilities occur, only the stellar mass necessary to restore stability is transferred from the disc to the bulge. No cold gas component is associated with the bulge in this model. In MORGANA, a significant fraction (half) of the baryonic mass (both gas and stars) of the disc is transferred to the bulge. This particular treatment avoids a series of consecutive instability events, that are instead frequent in the WDL08 model, in particular at high redshift. As we will show below, however, this modelling translates into a much more prominent role of the disc instability channel in bulge formation.

We stress that both models adopted for disc instabilities are oversimplified, and provide a very crude description of the complex phenomenology of bar formation and evolution. In particular, the WDL08 model neglects the possibility that bar formation produces an inflow of gas towards the centre that could fuel starburst/AGN activity, and that can eventually lead to bar disruption. The assumption of $V_{\text{disc}} = V_{\text{max}}$, as well as the use of only the stellar mass disk in Eq. 1 are questionable. On the other hand, MORGANA makes more realistic assumptions about the disc circular velocity and includes the gaseous mass present in the disc in Eq. 1. In both models, the outcome of an instability event is modelled in a rather arbitrary way. We note that present simulations do not provide clear indications about the fraction of disk mass that gets re-distributed, and how this depends on the halo/galaxy properties. In addition, the very criterion adopted to tag a disk as unstable has been questioned in recent studies (Athanasoula 2008). As we will show in the following, disk instability has important consequences on model predictions, and more work is certainly needed in

order to improve this aspect of our modelling. In order to quantify the importance of this process, in the following we will also show model predictions obtained when the disc instability channel is switched off. We will refer to these runs as the *pure mergers model* runs.

Another difference between the two models used in this study is given by how gas is treated during mergers. In the WDL08 model, the merger triggers a burst that converts a fraction of the combined gas into stars. These stars are added to the disc component of the remnant galaxy. In the MORGANA model, all gas and stars of the secondary are transferred to the bulge of the remnant galaxy, and the cold gas associated with the bulge is efficiently converted into stars.

Furthermore, we note that the WDL08 model accounts for satellite-satellite mergers, while MORGANA only considers mergers between satellites and central galaxies. Finally, the small differences in the cosmological parameters adopted in the two models have little impact on model predictions.

2.4 The Hopkins et al. prescriptions

Hopkins et al. (2009a, HOP09 hereafter) analyzed a suite of hydrodynamic merger simulations and derived a ‘gas-fraction dependent merger model’. We refer to the original paper for a detailed derivation of the model, while a summary of the key prescriptions can be found in Appendix A of Hopkins et al. (2009b). In this model, the fraction of cold gas that participates in the starburst associated with a merger can be written as:

$$f_{\text{burst}} = \frac{m_{\text{burst}}}{m_{\text{cold}}} = 1 - (1 + r_{\text{crit}}/R_d) \cdot \exp(-r_{\text{crit}}/R_d)$$

where

$$\frac{r_{\text{crit}}}{R_d} = \alpha \cdot (1 - f_{\text{gas}}) \cdot f_{\text{disc}} \cdot F(\theta, \mu) \cdot G(\mu)$$

and $f_{\text{gas}} = m_{\text{cold}}/(m_{\text{cold}} + m_{*,\text{disc}})$ is the gas disc fraction, $f_{\text{disc}} = (m_{\text{cold}} + m_{*,\text{disc}})/m_{\text{bar}}$ is the disc mass fraction, m_{bar} is the baryonic mass of the galaxy. R_d is the disc scale-length, and θ is the inclination of the orbit relative to the disc. Assuming that, before coalescence, the distance of pericentric passage is $b = 2 \cdot R_d$ (typical of cosmological mergers), one obtains:

$$\alpha F(\theta, \mu) = \frac{0.5}{1 - 0.42 \sqrt{1 + \mu \cos \theta}}$$

where the parameter α subsumes details of the stellar profile shape and bar driven distortion dynamics during a merger. Finally, $G(\mu)$ contains the dependence on the merger mass ratio, and has the form:

$$G(\mu) = \frac{2\mu}{1 + \mu}$$

where $\mu = m_2/m_1$. In the literature, and even in the two papers by Hopkins et al. mentioned above, there are inconsistencies in the definition of ‘mass-ratio’. In the implementation of the ‘Hopkins’ prescriptions used in this study, we define the mass of interest as the baryonic plus tightly bound central dark matter. Specifically, we have included the dark matter contribution in the following way: for each galaxy, we store the virial mass of the parent halo at the time of accretion (i.e. at the last time the galaxy is central), and add 10 per cent of this mass to the baryonic mass of the merging galaxies. We have verified, however, that the inclusion

of the dark matter contribution does not affect significantly the results discussed below. The new stars formed during the merger driven starburst are added to the bulge component of the remnant galaxy.

The whole stellar mass of the secondary is added to the spheroidal component of the remnant galaxy. It is further assumed that a fraction of the primary's stellar disc is transferred to the bulge component of the remnant galaxy, and is violently relaxed. Specifically, the mass of the disc that is 'destroyed' is:

$$m_{\text{disc,destroyed}} = \mu m_{*,\text{disc}} \quad (2)$$

We note that in the two standard models used in this study, the stellar disc of the primary is always unaffected during minor mergers and completely destroyed during major mergers. Therefore, we will monitor separately this model component when analysing results from the runs adopting these prescriptions.

Hopkins et al. (2009b) have investigated the implications of the proposed model in a cosmological framework, using both empirical halo-occupation models and the semi-analytic model presented in Somerville et al. (2008). In particular, they claim that their model leads to a significant suppression of bulge formation in low-mass galaxies, and that simulations and models that ignore the gas dependence of merger induced starbursts, have difficulties in reproducing the strong observed morphology-mass relation.

We have implemented the prescriptions illustrated above in both models used in this study, and will re-address these issues below. We note that in the runs adopting the HOP09 prescriptions, we have always switched off the disc instability channel. In addition, in the WDL08 model, the runs using these prescriptions assume that the stars formed during merger-driven starbursts are added to the bulge component of the remnant galaxy (as in Hopkins et al. 2009b). All other model details and parameters have been left unchanged.

3 DEPENDENCY ON STELLAR AND HALO MASS

In this section, we discuss the basic trends predicted by the two models used in this study, and analyze how they are modified by switching off the disc instability channel or adopting the HOP09 prescriptions discussed in the previous section.

Fig. 1 shows the median (stellar) bulge-to-total ratio as a function of the galaxy stellar mass, at four different redshifts. The left and middle columns show predictions from the WDL08 and MORGANA models, respectively, with different colours used for different physical assumptions. The right column compares predictions from the two models.

The WDL08 model (solid black lines) predicts a strong increase of the bulge-to-total ratio as a function of the galaxy stellar mass. When the disc instability channel for bulge formation is switched off (solid blue lines), the median bulge-to-total ratio decreases for all galaxies but the most massive ones which are still dominated by the bulge. Compared to

this pure mergers run, the HOP09 one² predicts a larger median bulge-to-total ratio for intermediate mass galaxies, but a smaller one for the most massive galaxies. In the WDL08 model, the median bulge-to-total at fixed stellar mass decreases slightly with increasing redshift. The scatter is large, as indicated by the shaded regions. This scatter is somewhat reduced when considering central galaxies only, and it reflects the variation in galaxy (and halo) merger trees at fixed galaxy stellar mass.

Also the standard MORGANA model (dashed black lines) predicts an increase of the median bulge-to-total ratio as a function of stellar mass, but this is somewhat shallower than that predicted by WDL08. In the pure mergers run (blue dashed lines), the median bulge-to-total ratio at fixed stellar mass decreases with respect to the standard run, but it is higher than in the corresponding run of the WDL08 model, particularly at high redshift. The HOP09 prescriptions provide predictions that are very close to those of the pure mergers model for intermediate mass galaxies, but again lower bulge-to-total ratios for the most massive galaxies. In the standard MORGANA run, the median bulge-to-total ratio increases slightly with increasing redshift, but with significant scatter at fixed stellar mass, as in WDL08.

The reason for the different behaviour obtained for intermediate mass galaxies when adopting the WDL08 version of the HOP09 prescriptions can be ascribed to the different treatment of merger driven starbursts in the WDL08 model: during minor mergers, new stars are added to the disc component of the remnant galaxy in the standard run, while to the bulge component in the HOP09 run (see Section 2.3). In contrast, in both the HOP09 and the pure mergers run of the MORGANA model, newly formed stars are added to the bulge component of the central galaxy.

Interestingly, the standard MORGANA run predicts a quite large bulge-to-total ratio for galaxies of all masses, even at $z \sim 2$, where a very large fraction of the galaxies have $B/T > 0.4$. Even in the pure merger run, most galaxies have $B/T > 0.2$ at this redshift, and the median bulge-to-total ratio is significantly higher than for WDL08 (compare blue dashed and solid lines in the bottom right panel of Fig. 1). Clearly, the efficient production of bulges in MORGANA at high redshift is not simply due to different assumptions made when the instability criterion is met, and is likely related to the shorter merger time scales adopted (De Lucia et al. 2010). We will come back to this issue later.

Fig. 2 shows the median bulge-to-total ratio as a function of the halo mass for the same redshifts as Fig. 1. The left and middle columns show results for each model only considering central galaxies, while the right column compares all results for satellite galaxies only.

Both models predict that a large fraction of central galaxies in haloes more massive than $\log[M_{\text{halo}}] \gtrsim 12.5$ are dominated by the bulge component (the fraction of bulge-dominated central galaxies is significantly larger for MORGANA than WDL08). In both models, the HOP09 prescriptions provide a somewhat weaker increase of the bulge-to-total ratio as a function of halo mass, and a reduction of the median bulge-to-total ratio for the most massive galaxies.

² We recall that the disc instability channel has been switched off in the run adopting the HOP09 prescriptions.

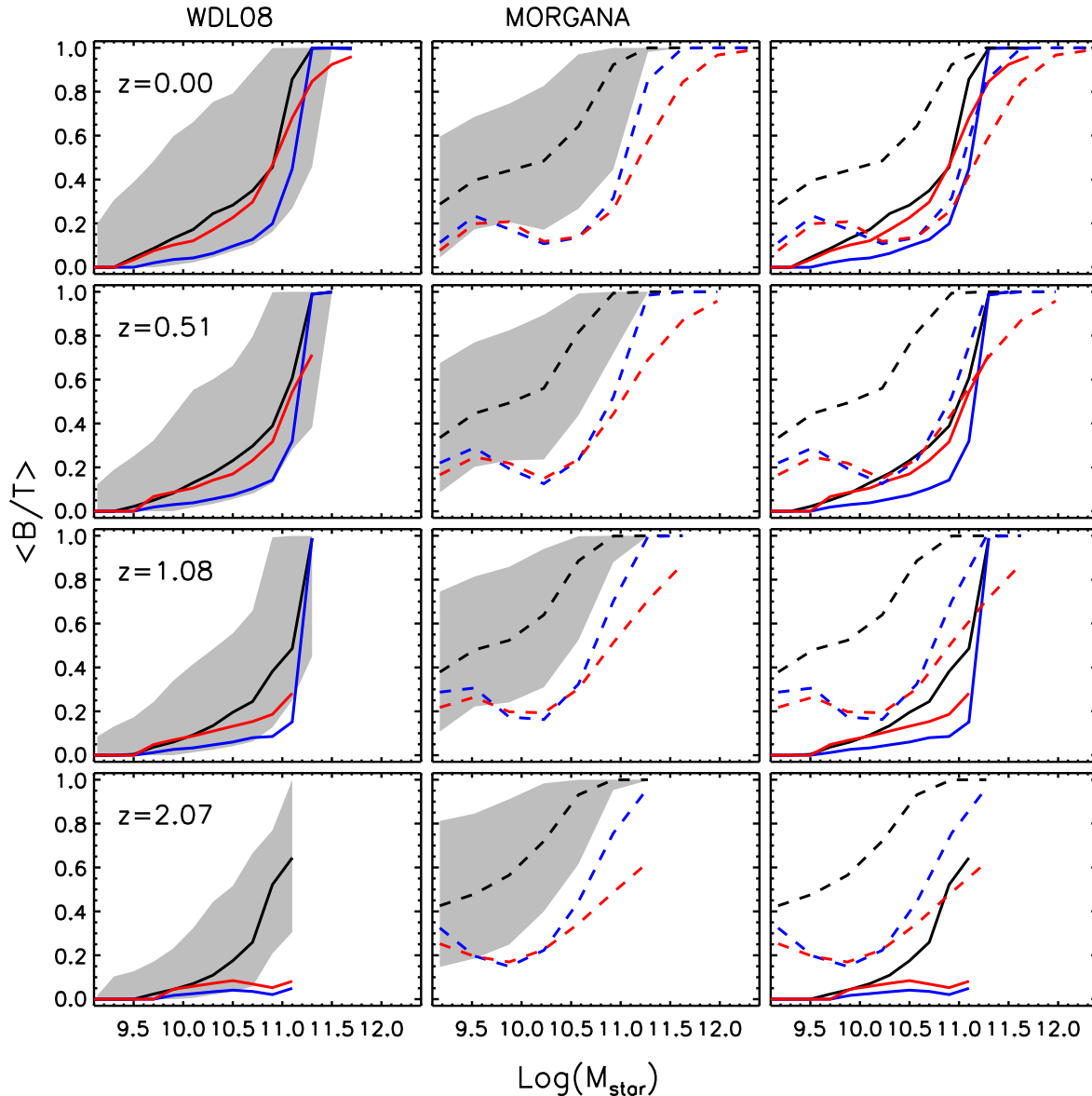


Figure 1. Median bulge-to-total ratio as a function of the galaxy stellar mass. Different rows correspond to different redshifts, while different columns correspond to different models: the left column shows results from the WDL08 model; the middle column shows results from MORGANA, and the right column compares results from the two models. In all panels, black lines correspond to the standard models, blue lines correspond to the pure merger variant of these models, and red lines show results obtained using the HOP09 prescriptions. The shaded regions in the left and middle columns show the 15th and 85th percentiles of the distributions obtained for the standard WDL08 and MORGANA runs respectively.

The scatter at fixed halo mass is large, reflecting significant variations in the accretion histories of haloes (and of their central galaxies) at fixed mass.

The median bulge-to-total ratio of satellite galaxies is relatively low (lower in the WDL08 model than in MORGANA), and approximately constant as a function of halo mass. We note that, in these models, once a galaxy is accreted onto a larger system (i.e. becomes a satellite galaxy) its bulge-to-total ratio is unaffected, unless it suffers a

merger with another satellite galaxy³. In the real Universe, tidal stripping and interactions with other satellite galaxies (e.g. harassment) are likely to increase the bulge-to-total ratio of satellite galaxies, increasing the median values plotted in Fig. 2.

Interestingly, almost all central galaxies in haloes with mass slightly larger than $\sim 10^{12} M_{\odot}$ are practically ‘pure bulges’ in the MORGANA model, and the vast majority

³ Mergers between satellites are included in WDL08 but not in MORGANA.

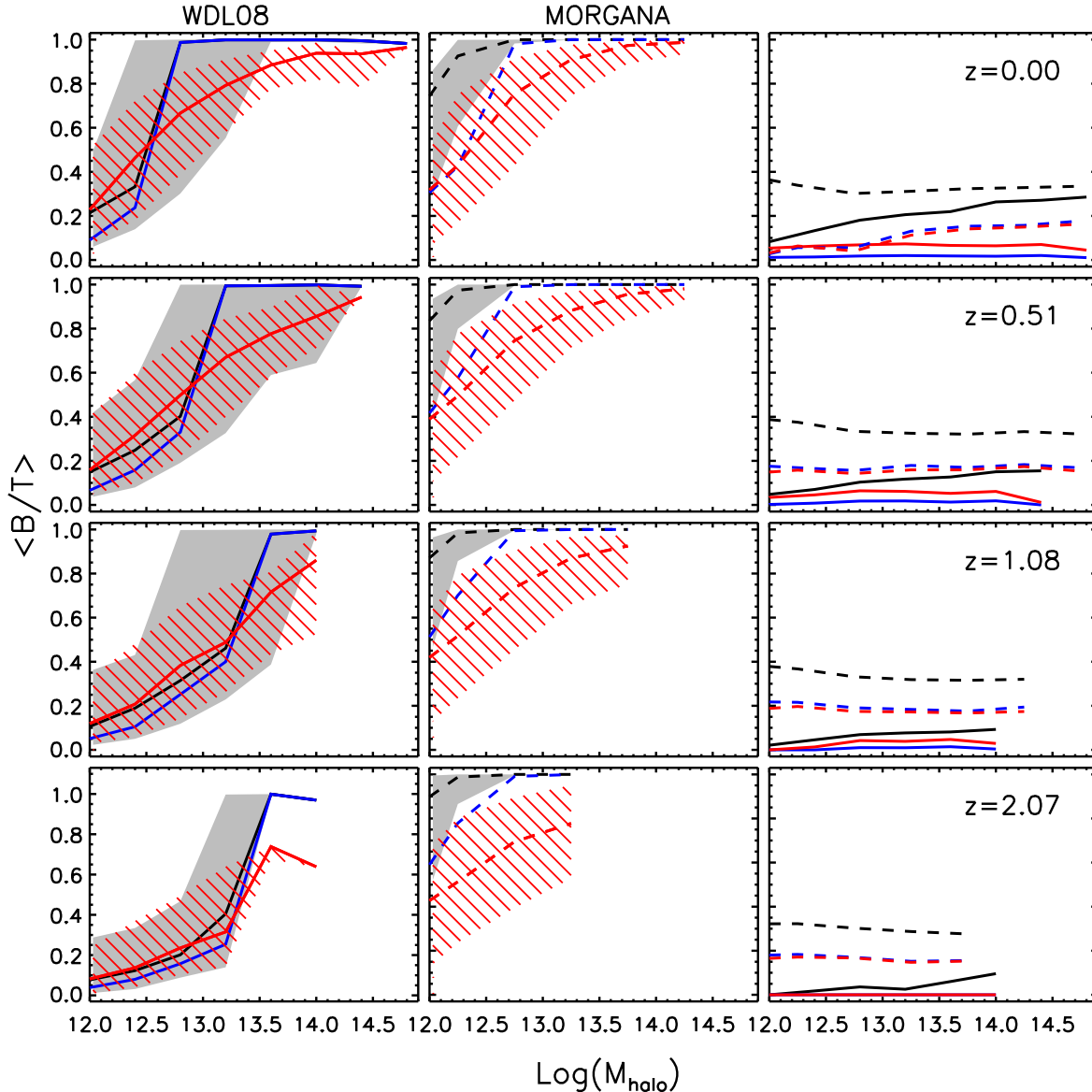


Figure 2. Median bulge-to-total ratio as a function of the parent halo mass. Different rows correspond to different redshifts, while different columns and colours correspond to different models, as in Fig. 1. The left and middle columns have been obtained for central galaxies only, while the right column compares results for satellite galaxies. The shaded regions in the left and middle columns show the 15th and 85th percentiles of the distribution for the standard and HOP09 runs.

of central galaxies in ‘Milky-Way type haloes’ (with mass $\sim 10^{12} M_{\odot}$) have $B/T > 0.6$, at all redshifts considered. These results suggest that the standard MORGANA run has difficulties in forming a Milky-Way like galaxy in haloes of mass similar to that of our Galaxy⁴. This does not appear to be a problem in the standard WDL08 run (see also De Lucia & Helmi 2008; Li et al. 2010). We note, however, that haloes of this mass are only marginally resolved in the

⁴ Macciò et al. (2010) have studied predictions from MORGANA for the luminosity function of ‘Milky-Way’ satellites. However, in the version of the model they use, the disc instability channel is switched off.

simulations used in this study (with ~ 1000 particles in the WDL08 simulations).

4 HOW AND WHEN DO BULGES FORM?

The models we have in hands allow us to ask a number questions about the formation of bulges: when did bulges form? Was most of their mass assembled during major or minor mergers? What is the relative importance of disc instability? How does this vary as a function of redshift? And in which environments did bulges form?

In order to answer these questions, we have rerun our models and, each time the mass of the bulge is updated,

we have stored the information about the redshift, the halo mass and the fraction of mass contributed to the final bulge, distinguishing between major mergers, minor mergers, and disc instability. For the runs that use the HOP09 prescriptions, where we do not include the disc instability channel, we have stored separately the information about the bulge mass contributed through destruction of the primary’s stellar disc (e.g. Eq. 2 in Section 2.4). We note that our definition of bulge formation refers to the event adding stars to the bulge of the selected galaxy or its main progenitor, i.e. the clock is reset for stars in a secondary galaxy once it merges with a more massive one.

The ‘channels’ defined above correspond generally to a combination of different physical processes: e.g. in MOR-GANA, disc instability triggers both a re-arrangement of the stellar material originally distributed in the disc, and the inflow of disc gas towards the centre. This leads, in turn, to the formation of *in situ* new stars - a process that is not included in the WDL08 treatment of disc instability. Analogously, mergers are generally associated with both a starburst, and a re-arrangement of stars belonging to the merging galaxies.

Fig. 3 shows the fraction of bulge mass contributed through different channels (different columns) for galaxies selected at $z = 0$ as those having $B/T > 0.4$ (qualitatively, the results do not change significantly when considering all galaxies). We have split model galaxies into four stellar mass bins, and show the corresponding results in different rows, with the most massive galaxies shown at the bottom. As in previous figures, solid lines show results from the WDL08 runs, while dashed lines show the corresponding results from MOR-GANA, with different colours referring to different runs. Where a black line is not visible, it overlaps perfectly with the corresponding blue line, meaning that switching off disc instability does not affect the contribution of that particular channel to the final bulge mass (bottom panels). In the right column, the black lines show the fraction of bulge mass formed through the disc instability channel in the standard models, while red lines correspond to the fraction of bulge mass formed through destruction of the primary’s disc in the runs that adopt the HOP09 prescriptions. We stress that these two sets of lines have been plotted in the same panels for convenience, and should not be compared against each other.

Fig. 3 shows that the contribution from major mergers decreases with increasing stellar mass, while the contribution from minor mergers increases. The contribution from disc instability is largest for intermediate-mass galaxies, and negligible for the most massive galaxies considered (bottom right panel). Both models and all runs considered share these trends, with a few notable differences: (i) bulges seem to form earlier in MOR-GANA than in WDL08; (ii) the contribution from disc instability is larger in the MOR-GANA model. For the most massive galaxies, disc instability contributes less than ~ 1 per cent of the final bulge mass, and all instabilities occurred at high redshift, in the small galaxies that later merged to form these massive systems. In MOR-GANA, the contribution from the disc instability channel is ~ 3 per cent for the most massive galaxies, but it tends to increase (weakly) since $z \sim 4$. These results can be compared to those that Parry et al. (2009) find for the semi-analytic model discussed in Bower et al. (2006). Their

Figure 8 shows that instabilities contribute to the bulges of present day galaxies significantly more than minor and major mergers, but for the most massive galaxies where the major merger contribution is dominant. Interestingly, they show that the contribution from disk instabilities in the ‘Durham’ model is much larger than that in the ‘Munich’ model (which corresponds to the WDL08 model used in this study). The large contribution from disk instabilities in the Durham model is noted also in Benson & Devereux (2010, see e.g. their Figure 5), and is due to the assumption that instabilities result in the complete collapse of the disc (both of its stellar and gaseous component - see original paper for details). Clearly, the different outcome assumed for instability events has important consequences on the relative importance of different channels to bulge formation - a conclusion that seems to contradict what found by Benson & Devereux (2010, appendix A2). We will come back to this issue later.

In MOR-GANA, the HOP09 prescriptions result in a contribution from major and minor mergers that is approximately equal to that found in the standard run. In the WDL08 model instead, the HOP09 prescriptions result in a systematically lower contribution from major mergers, and higher contribution from minor mergers, at all redshifts. This is largely due to the fact that, when adopting the HOP09 prescriptions, the WDL08 model assumes that the stars formed during all merger driven starbursts are added to the bulge component of the remnant galaxy (rather than to the disc in the case of minor mergers, as in the standard run). The reduced contribution from major mergers relates partly to the increased efficiency of bulge formation via minor mergers. One notable consequence of the HOP09 prescriptions for the WDL08 model is for the most massive galaxies considered: for these, the major mergers channel becomes important only at $z < 1$. Finally, in both models, the disc destruction channel contributes significantly to the final bulge mass for the intermediate mass bins considered, but less than 10 per cent for the most massive galaxies in the sample.

As mentioned above, the merger model adopted in MOR-GANA provides galaxy merger times that are systematically lower than those used in the WDL08 (De Lucia et al. 2010). Since a significant fraction of the final bulge mass is associated with galaxy mergers (both minor and major), systematic differences between the galaxy merger time-scales are expected to lead to a systematic difference in the characteristic formation times of galactic bulges. In order to understand how these differences affect the results discussed above, we have re-run the MOR-GANA models using the same dynamical friction timescale prescriptions adopted in WDL08. Results are shown in Fig. 4. We note that residual merger times are assigned at the time of halo mergers in MOR-GANA, and orbital parameters are re-assigned after each major merger. In WDL08, residual merger times for satellite galaxies are instead assigned when the parent dark matter substructures are stripped below the resolution limit of the simulation. So, although we are using now the same formulation of dynamical friction in the two models, overall merger times will still be different.

The figure shows that, when using longer merger times for the MOR-GANA runs, bulges form later, particularly for the most massive galaxies considered. Interestingly, making merger time-scales longer also increases the contribu-

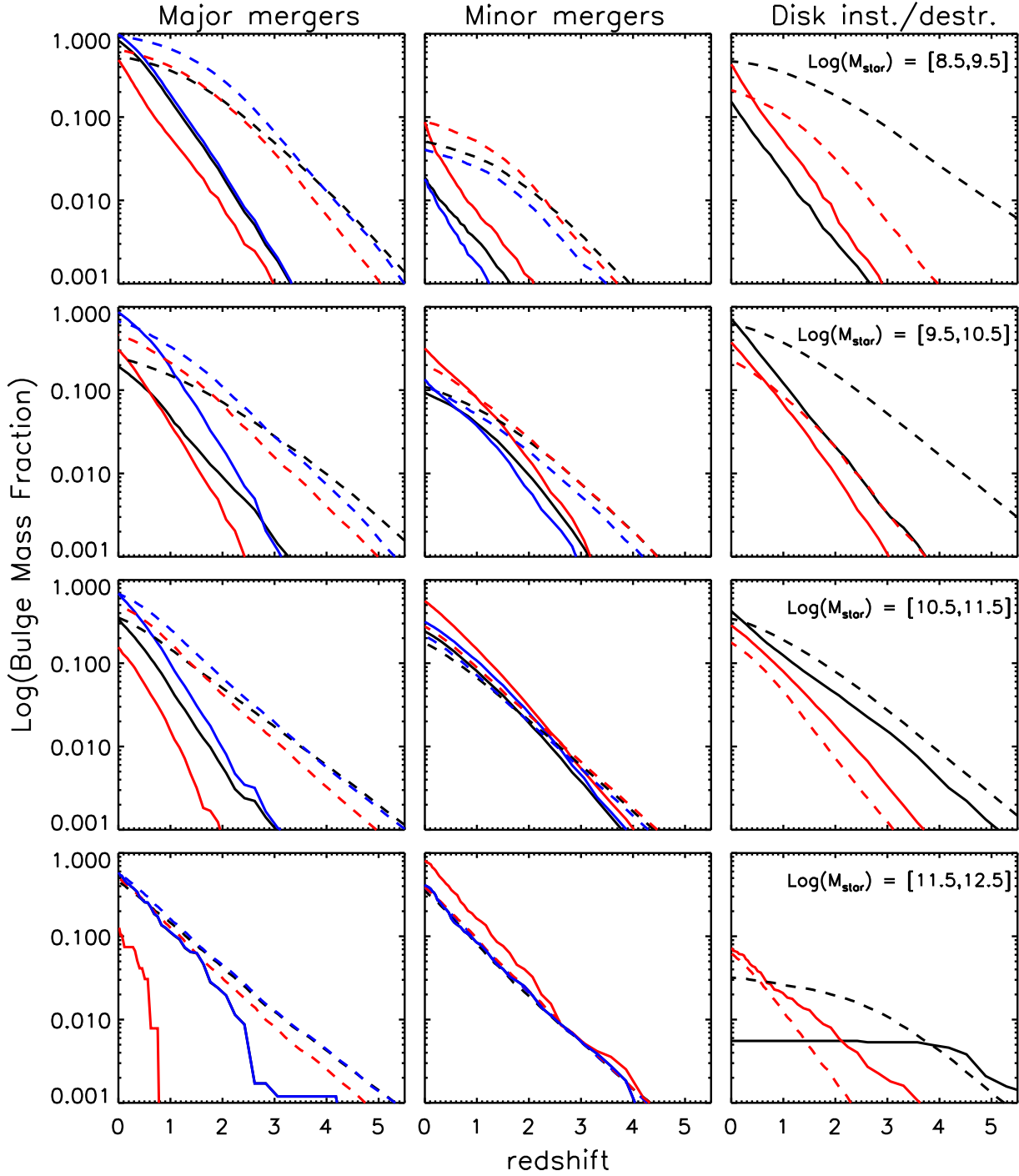


Figure 3. Fraction of bulge mass formed as a function of redshift through different channels (different columns), for galaxies with $B/T > 0.4$ selected at $z = 0$. Different rows correspond to different stellar mass bins, while different colours and linestyle correspond to results from different models as in Fig. 1. Where a black line is not visible, it overlaps perfectly with the corresponding blue line. In the right column, the black lines indicate the fraction of bulge mass formed through disc instability in the standard run, while red lines correspond to the fraction of bulge mass formed through destruction of the primary’s stellar disc in the HOP09 prescriptions (see Eq. 2 in Section 2.4).

tion from disc instability in the standard MORGANA run. This happens because galaxy discs now have longer times to develop instabilities. Increasing the merger times in MORGANA does not account for all differences between the two models used in this study. In particular, bulge formation still

occurs earlier in MORGANA than in WDL08 for intermediate to low mass galaxies, and disc instability plays a much more important role in MORGANA than in the WDL08 model, particularly at high redshift.

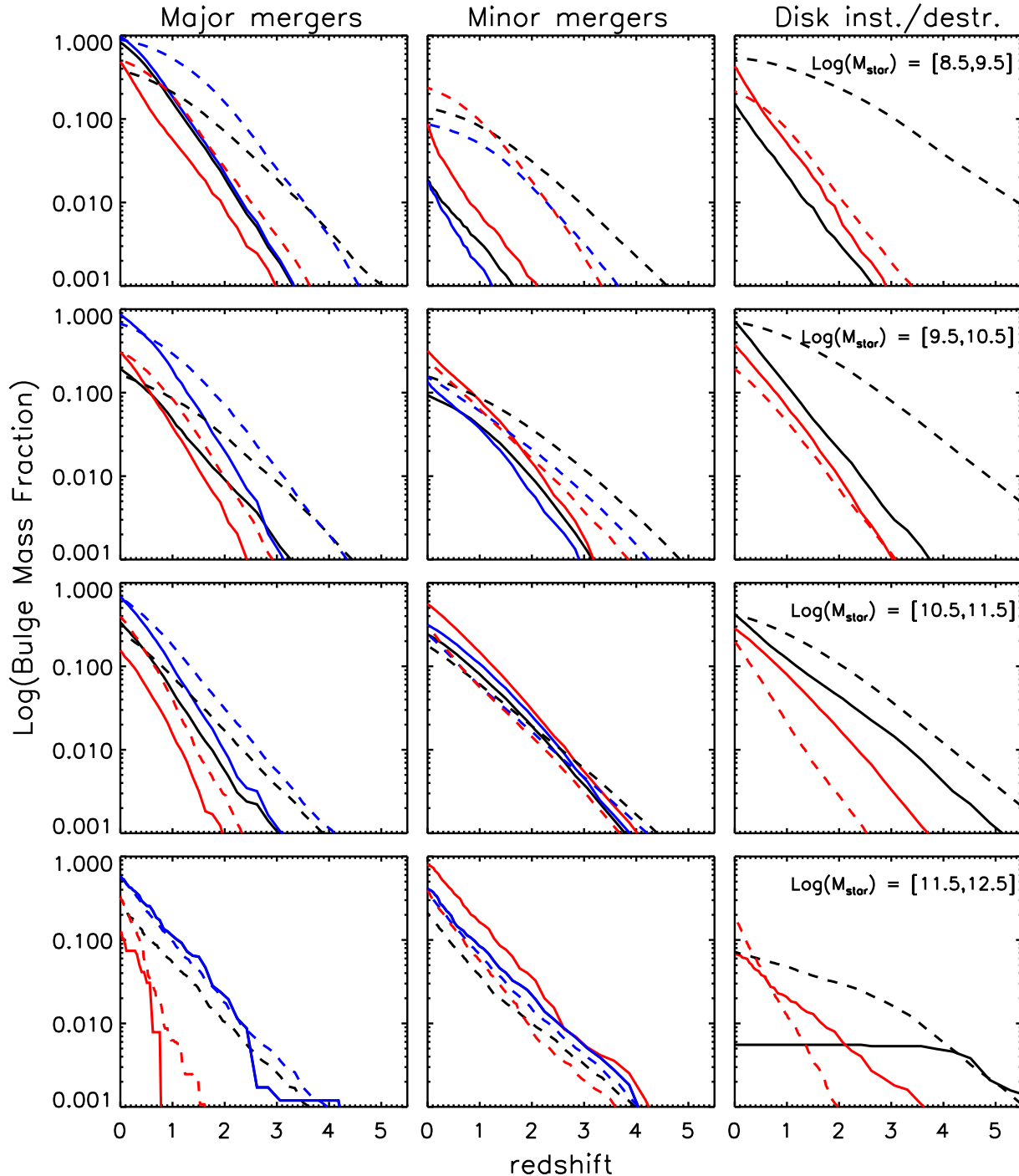


Figure 4. As in Fig. 3, but using longer merger times in the MORGANA runs (see text for details).

5 HOW AND WHERE DO BULGES FORM?

In the previous section, we have analyzed *when* bulge formation occurs, and what is the relative importance of different channels at different times. Another question that can be addressed with our models is: what is the typical *environment* of bulge formation? Does it occur in groups or in the ‘field’? And how does the characteristic environment of bulge formation vary as a function of cosmic time?

In Figs 5 and 6, we show the fraction of bulge mass

contributed through different channels, as a function of redshift and parent halo mass, for the WDL08 and MORGANA models respectively. Different rows correspond to different present day stellar mass bins, while different columns refer to different channels, as indicated by the legend. Data shown in Figs 5 and 6 have been computed for the standard model considering all galaxies with $B/T > 0.4$, and have been normalized to the total bulge mass in each mass bin. Therefore, darker regions in each panel of Figs 5 and 6 indicate the ranges of redshift and halo mass where that

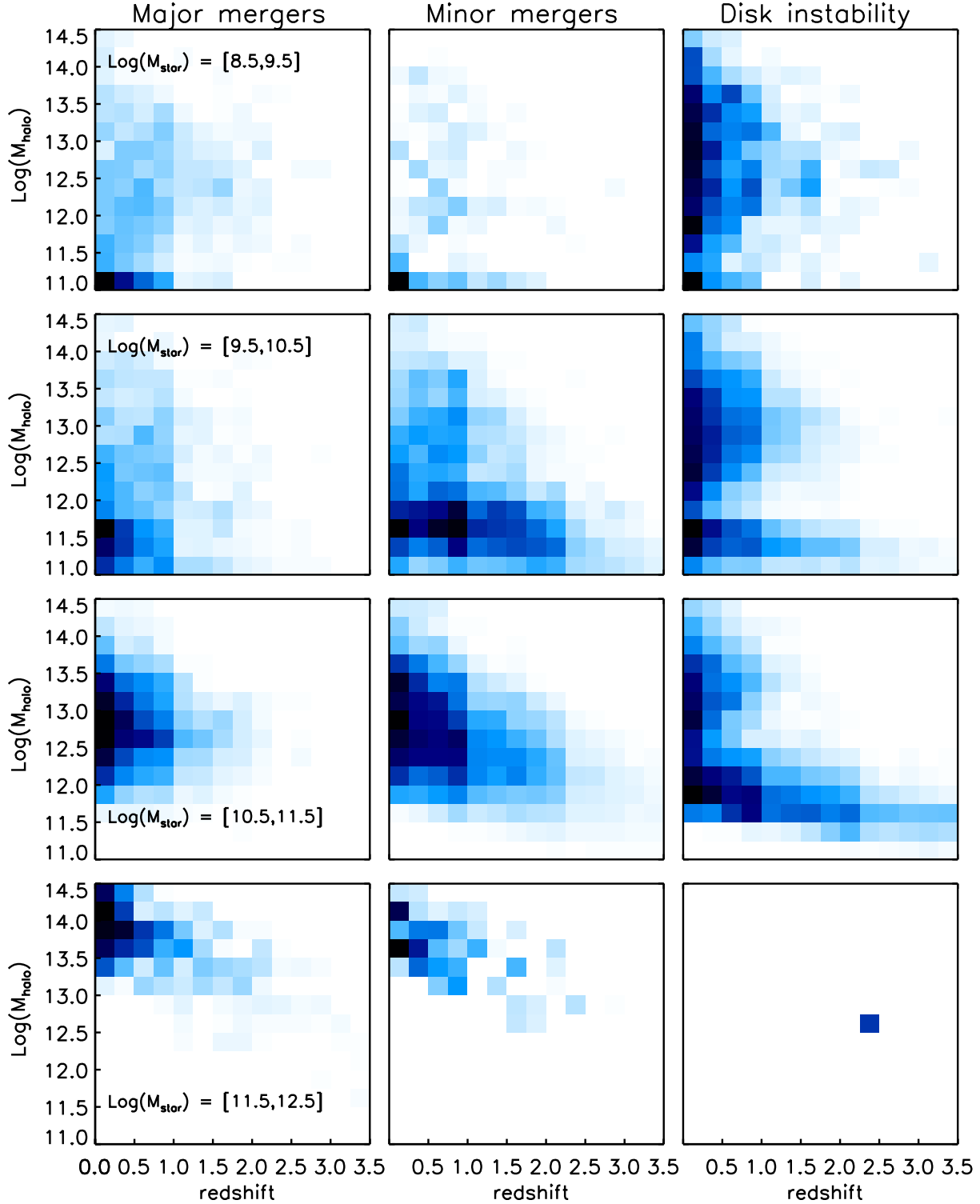


Figure 5. Fraction of the total bulge mass of galaxies of different stellar mass (increasing from top to bottom row) contributed from different channels (different columns), as a function of redshift and parent halo mass. For the standard WDL08 run.

particular channel is more important. Qualitatively, the results shown do not change when including all galaxies (i.e. without any cut for the bulge-to-total ratio).

The figures show that the typical halo mass where different processes contribute to bulge formation increases

with increasing stellar mass. Interestingly, for galaxies with $\log[M_{\text{star}}] \sim 9 - 10$, much of the bulge formation occurs in haloes of $\log[M_{\text{halo}}] < 11.5$ that are only marginally resolved in the simulations used in this study. One clear difference between the two models is that bulge formation occurs

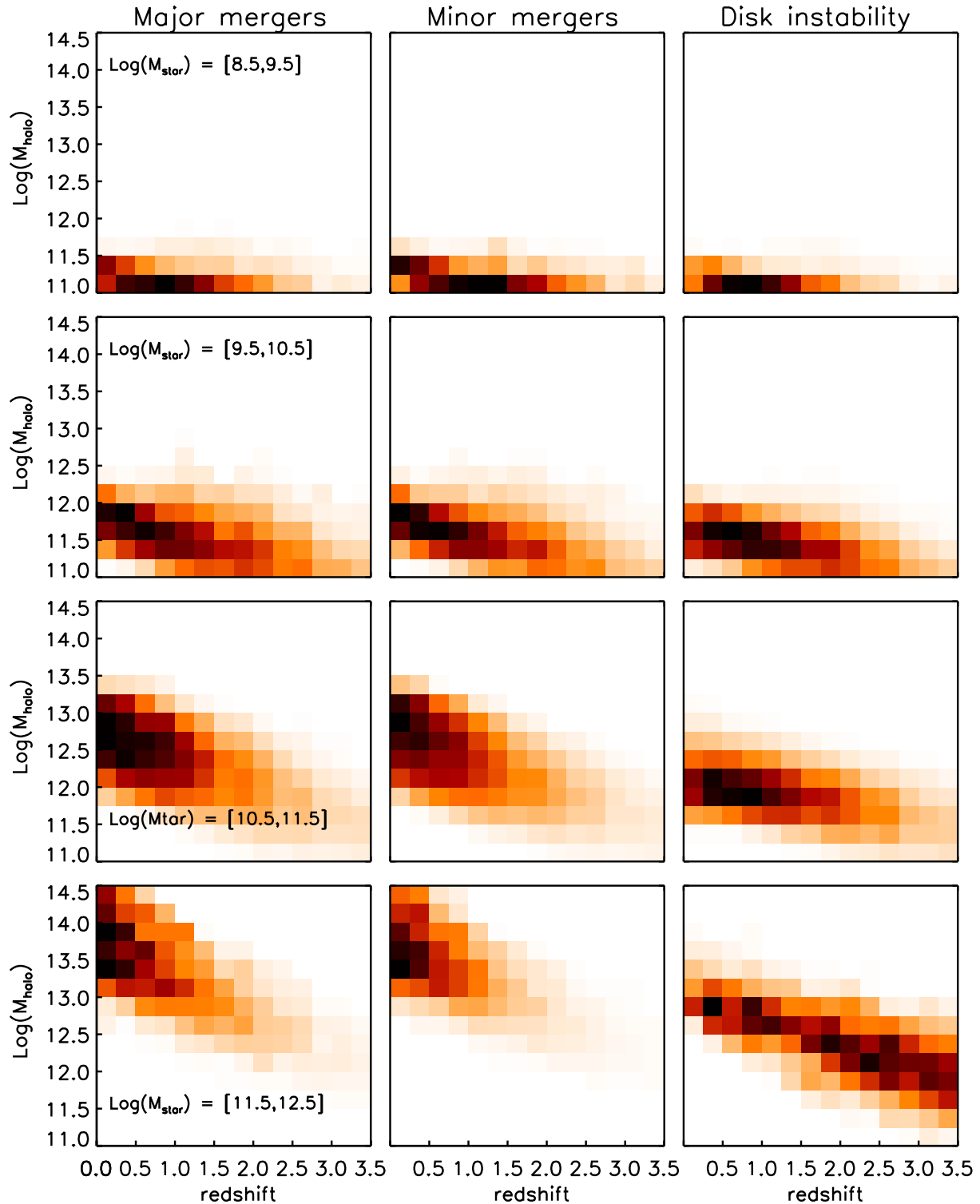


Figure 6. Same as in Fig. 5, but for the standard MORGANA run.

on a wider range of halo masses (more extended towards larger masses) in WDL08. This difference is primarily seen for satellite galaxies. Indeed, when excluding these galaxies, Figs 5 and Fig. 6 become more similar. For the major and minor mergers channels, this difference is due to the fact that the WDL08 model takes into account mergers be-

tween satellite galaxies, that are not included in MORGANA. The contribution from satellite galaxies to the disc instability channel comes from the fact that in WDL08, the disc radius of a satellite decreases in proportion to the radius of its dark matter halo. This might not be generally true and could artificially increase the bulge-to-total ratio of satellite

galaxies. We have verified that fixing the disk radius at the time of infall⁵ decreases significantly the contribution from disk instability due to satellite galaxies. We note, however, that our model does not include physical processes such as tidal stripping and harassment that would again increase the bulge-to-total ratio of satellites.

Another obvious difference between Figs 5 and 6 is the more pronounced (and extended) contribution from disc instability to the formation of the most massive bulges in the standard MORGANA run with respect to the WDL08 model (see also bottom right panel of Fig. 3). Finally, these figures show that there is a somewhat ‘tighter’ correlation between the mass of the halo and the redshift in MORGANA. This is likely due to the fact that mass accretion histories obtained using PINOCCHIO are ‘smoother’ than those obtained from numerical simulations.

6 ELLIPTICALS AND DISC REGROWTH

In this section, we will focus on galaxies that are dominated by a bulge, and that we will call ‘ellipticals’ (for a more extended discussion on the formation history of elliptical galaxies, see also De Lucia et al. 2006)⁶. More specifically, we include in the elliptical class all galaxies with at most ten per cent of the stellar mass in a disc ($B/T > 0.90$). We will address, in particular, three specific questions: (i) what is the typical stellar mass and environment of elliptical galaxies? (ii) what is the frequency and relevance of disc regrowth for these galaxies? (iii) when do galaxies *become ellipticals* and through which physical process(es)?

Fig. 7 shows the fraction of galaxies classified as ellipticals, as a function of the galaxy stellar mass (left panels) and of the parent halo mass (right panels). Top and bottom panels refer to the WDL08 and MORGANA models, respectively. As the stellar mass increases, a larger fraction of galaxies are classified as ellipticals, and the distributions computed from MORGANA extend to larger masses than those obtained for WDL08. We note that an excess of massive galaxies in the MORGANA model is well documented and is primarily due to an inefficient suppression of star formation in central galaxies by AGN feedback (e.g. Fontanot et al. 2009; Kimm et al. 2009). Disc instability does not affect significantly the number and distribution of elliptical galaxies in WDL08, while the fraction of ellipticals is sensibly reduced when switching off the disc instability channel in MORGANA, also at relatively large masses. The distribution as a function of halo mass is approximately flat for the WDL08 model, and more skewed towards low-mass haloes in MORGANA (i.e. a larger fraction of galaxies residing in relatively low-mass haloes are classified as ellipticals in this model), where a large fraction of ellipticals in relatively low-mass haloes form through disc instability. The decreasing fraction to higher halo mass in this model is due to the increasing contribution of disc-dominated satellite galaxies.

⁵ Weinmann et al. (2010) have verified that results from the model would be virtually unchanged but for the morphology of satellite galaxies.

⁶ Note, however, that a different definition of ‘ellipticals’ was adopted in that study.

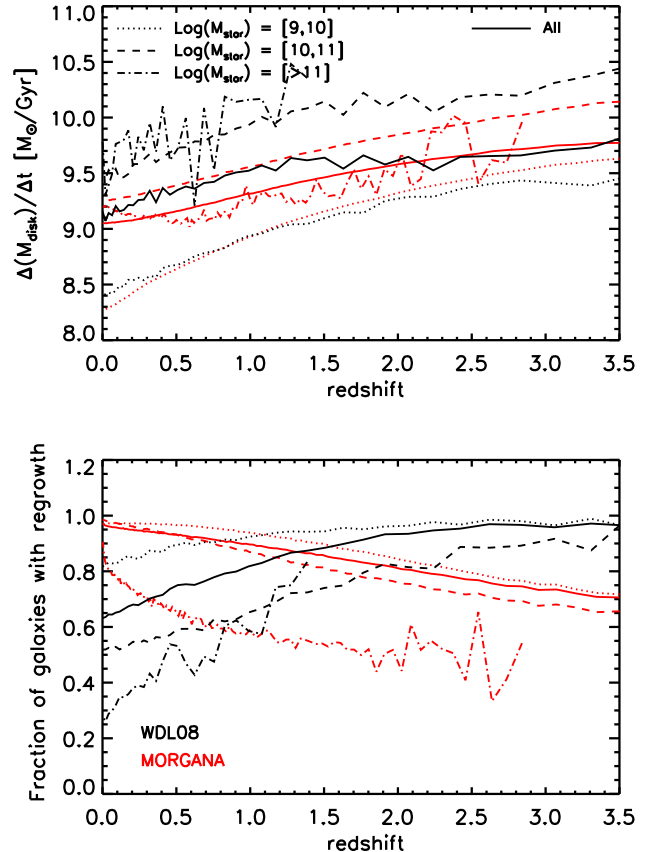


Figure 8. Top panel: Mean regrowth rate (see text for details). Bottom panel: fraction of central galaxies that regrow a disc. Black lines refer to the standard WDL08 run, while red lines correspond to the standard MORGANA run. Different line styles correspond to galaxies of different stellar mass, as indicated in the legend.

Interestingly, the HOP09 prescriptions tend to reduce significantly the number of ellipticals in both models. Overall, the number densities of galaxies that are classified as ellipticals in MORGANA are much larger (more than a factor two) than those obtained in WDL08. We note that model results are in qualitative agreement with observational data indicating that the total fraction of ellipticals is not expected to be higher in more massive haloes (Wilman et al. 2009).

As discussed in Sections 2.1 and 2.2, bulge dominated galaxies can regrow a new disc, provided there is enough cooling from the surrounding hot halo gas. In principle, minor mergers with gas-rich satellites also form new disc stars in the WDL08 model. However, most of the galaxies accreted onto centrals of relatively massive haloes (where most of the central ellipticals are) will be gas-poor (De Lucia & Blaizot 2007), and mergers between satellites are rare. Therefore, the only mechanism through which galaxies can grow a new disc is by accretion of fresh gas material from the surrounding hot halo.

In order to quantify the importance of disc regrowth, we have selected all central elliptical galaxies from our models and analyzed their merger trees, storing the increase of their

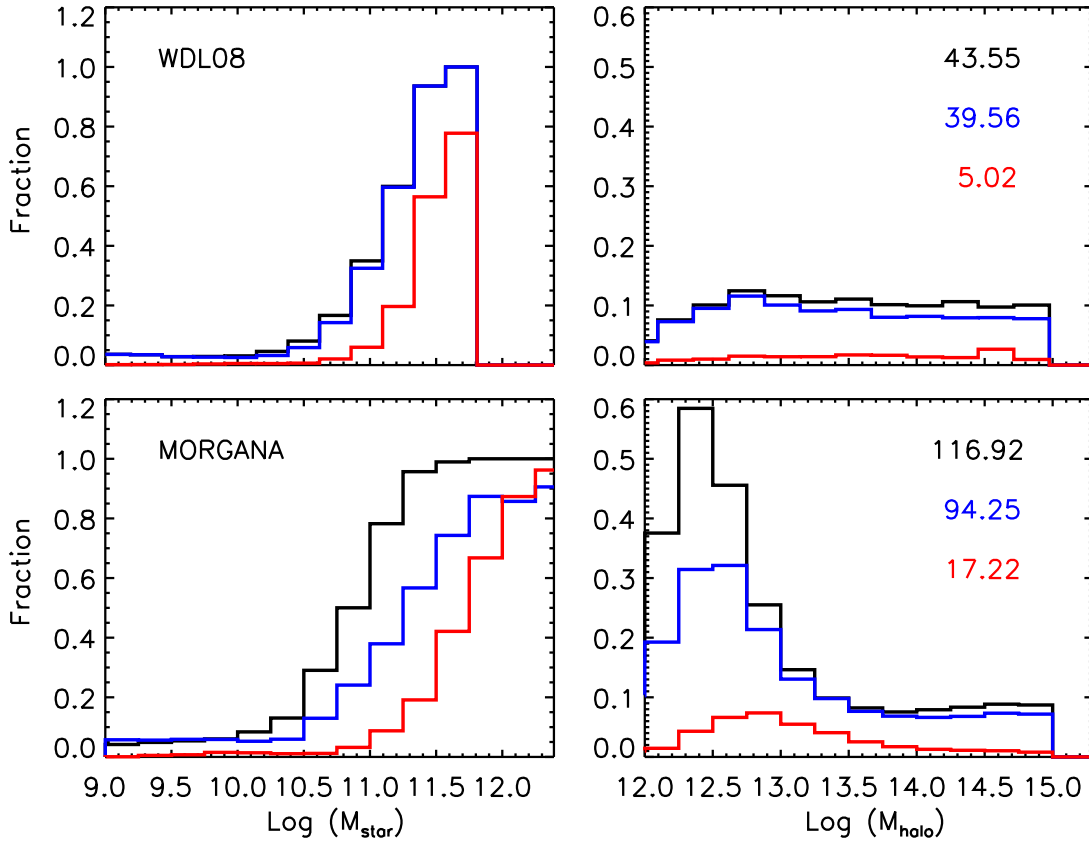


Figure 7. Distribution of galaxies with $B/T > 0.90$ at $z = 0$, as a function of the galaxy stellar mass (left panels) and of the parent halo mass (right panels). The top and bottom rows show results for the WDL08 and MORGANA models respectively. Different colours correspond to different runs: black lines correspond to the standard models, blue lines correspond to the pure mergers variant of these models, and red lines show results obtained using the HOP09 prescriptions. The number densities of galaxies are given in the legend of the right panels, and are expressed in units of Mpc^{-3} . The histograms have been normalized dividing by the number of galaxies in each stellar or halo mass bin.

stellar disc mass as a function of time, until they become satellites (or until $z = 0$, for central galaxies). The top panel of Fig. 8 shows the mean regrowth rate for galaxies in different stellar mass bins (the stellar mass corresponds to that of the galaxy at the redshift under consideration). The rates shown in Fig. 8 have been normalised to the total number of (central) galaxies experiencing regrowth. The figure shows that, on average, the rate of disc regrowth decreases with decreasing redshift, for galaxies of all masses. For the most massive galaxies considered (dot-dashed lines in Fig. 8), the rate of regrowth averaged over 1 Gyr time-scale is always significantly smaller than the galaxy mass at the corresponding time. This means that a galaxy that crosses the threshold $B/T = 0.90$ when it is already rather massive, will likely stay above this threshold at any later time. For lower mass galaxies, the rates are more significant, particularly at high redshift where galaxies are more gas-rich. On average, however, these galaxies will not grow a large disc: a galaxy with stellar mass $\sim 10^{10} M_{\odot}$ and $B/T = 1$ will regrow a disc containing about 10 per cent of the mass in $\sim 3 - 7$ Gyr at $z \sim 0$, or $\sim 1 - 3$ Gyr at $z \sim 1$. Disc regrowth is also inhibited by subsequent mergers which increase the bulge-to-total ratio. These results suggest that disc regrowth is not significant for the most massive galaxies, but that it repre-

sents a non negligible component in the evolution of low and intermediate mass galaxies, particularly at high redshift.

The bottom panel of Fig. 8 shows the fraction of central galaxies experiencing regrowth in the two models used in this study. At the highest redshifts considered, the balance between cooling and feedback is such that more galaxies grow a disc in WDL08 than in MORGANA. As the redshift decreases, AGN feedback becomes more and more important, particularly for the most massive galaxies (that are sitting in the most massive haloes). This determines a significant decrease of the fraction of central galaxies experiencing regrowth in WDL08: only about 20 per cent of the most massive galaxies are growing a new disc, and, as explained above, this occurs at relatively low rates. On the contrary, the fraction of central galaxies experiencing disc regrowth *increases* with decreasing redshift in MORGANA. Albeit the regrowth rates are low also in this model, almost all galaxies (~ 90 per cent of the most massive ones) are growing a new disc. This different behaviour can be ascribed to the different treatment of radio-mode AGN feedback, that is much more efficient in suppressing cooling in WDL08 than in MORGANA (e.g. Kimm et al. 2009; Fontanot et al. 2010).

Another interesting question to address about elliptical galaxies is when and through which mechanism(s) they ac-

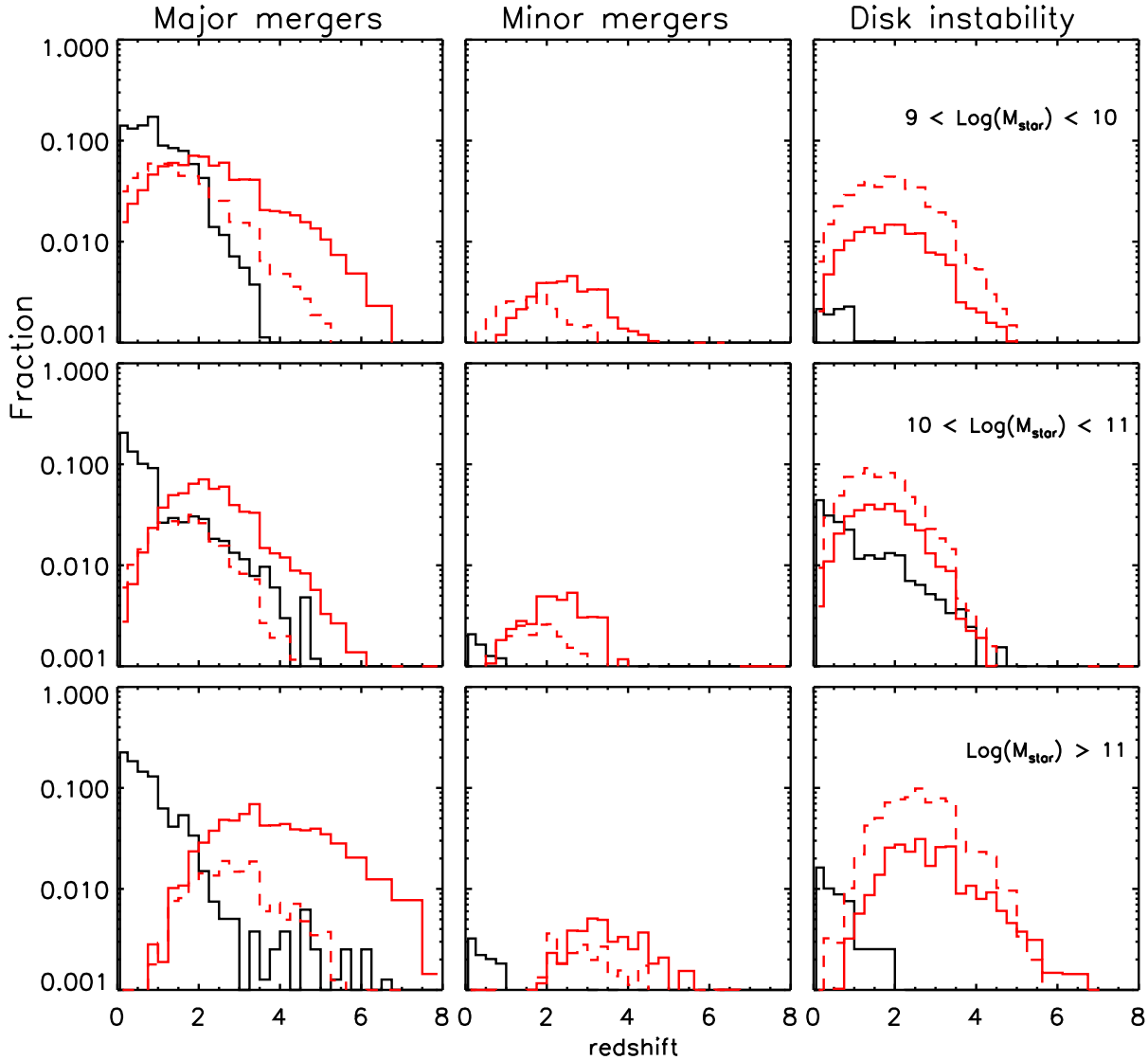


Figure 9. Distribution of the times when galaxies cross the threshold $B/T = 0.9$ for the first time. Galaxies are split by their final stellar mass (different rows) and each column shows the contribution from different channels. Galaxy counts are weighted by the fraction of bulge mass contributed by each process, and histograms are normalised by the total number of galaxies in each mass bin. Black and red lines are used for the WDL08 and MORGANA model, respectively. Red dashed lines show results obtained from MORGANA using longer merger times.

quired their morphology. We address this question in Fig. 9 where we show the redshift at which galaxies cross the threshold $B/T = 0.9$ for the first time. Galaxies are split by their final mass and different columns correspond to different bulge formation channels. When several processes contribute to make the galaxy cross the threshold $B/T = 0.9$, we have weighted the counts by the fraction of bulge mass contributed by each channel. The figure shows that most galaxies acquire an ‘elliptical’ morphology because of a major merger event (left column), while minor mergers seem to play a negligible role in turning galaxies into ellipticals, particularly in WDL08. Disc instability is responsible for turning a relatively large fraction of galaxies into ellipticals in MORGANA, particularly at intermediate masses, while it plays a much less prominent role in WDL08. The distributions obtained from MORGANA are peaked at redshifts significantly higher than in WDL08, as a consequence of the

significantly shorter merger times and of the more prominent role of disc instability. Dotted lines in Fig. 9 show results from MORGANA obtained adopting longer merger times (see Section 4), and confirms that galaxies become ellipticals later when longer merger times are adopted. As discussed in Section 4, the figure also shows that this run is characterized by a larger contribution from disc instability to bulge formation. We stress that the times plotted in Fig. 9 should not be confused with the ‘formation times’ of elliptical galaxies, as these times are not related to the star formation history of these galaxies.

Not all galaxies considered in Fig. 9 are still ellipticals at $z = 0$. As discussed above, however, the regrowth rates are lower for intermediate-massive galaxies so that a larger fraction of the most massive galaxies maintain their elliptical morphology down to $z = 0$. In particular, we find that in the WDL08 model about 30, 64, and 96 per cent of the galaxies

in each of the mass bins considered (in order of increasing mass) still have $B/T > 0.9$ at redshift zero. In MORGANA, the corresponding fractions are 85, 46, and 88 per cent. The fractions increase to about 53, 79, and 98 for the WDL08 model and 89, 61, and 92 per cent for MORGANA, when considering galaxies with $B/T > 0.6$ at $z = 0$.

7 DISCUSSION AND CONCLUSIONS

In this paper, we have analyzed predictions for the formation of bulges from two independently developed galaxy formation models. In particular, we have considered (i) the recent implementation of the Munich model (WDL08) by De Lucia & Blaizot (2007), with its generalization to the WMAP3 cosmology discussed in Wang et al. (2008), and (ii) the MORGANA model presented in Monaco, Fontanot & Taffoni (2007), and adapted to a WMAP3 cosmology as described in Lo Faro et al. (2009).

The two models include the same channels for bulge formation (mergers and disc instability), but assume different prescriptions to model these physical processes. In order to study how results vary as a function of specific physical assumptions, we have also implemented alternative merger prescriptions (Hopkins et al. 2009), based on results from recent hydrodynamic merger simulations. In this paper, we have focused on theoretical predictions, postponing to a forthcoming paper a detailed comparisons with observational results (Wilman et al., in preparation). In a companion paper (Fontanot et al., in preparation), we will study the physical properties and formation histories of galaxies with no significant bulge component, as predicted by the same models considered here.

Both models used in this study, with all different physical assumptions considered, predict a strong correlation between the galaxy morphology and its stellar mass, with more massive galaxies having larger bulge-to-total ratios. For central galaxies, there is also a strong correlation between the morphology of a galaxy and its parent halo mass, with most of the central galaxies of haloes with mass larger than $\sim 10^{13} M_{\odot}$ being dominated by a bulge. These trends are not surprising, given our assumption that bulges form during mergers, and the strong correlation between the galaxy mass and the mass of the parent halo for central galaxies: more massive galaxies will generally have a richer merger history than their less massive counterparts, and more massive galaxies will sit at the centre of more massive haloes.

Taking advantage of our models, we have studied in detail the contribution to bulge formation from different ‘channels’ (major and minor mergers, and disc instability). Differences arise between the different models and implementations, but the results at redshift zero can be summarized as follows:

- (i) major mergers dominate the contribution to bulges of galaxies less massive than $\sim 10^{10} M_{\odot}$;
- (ii) for galaxies more massive than $\sim 10^{10} M_{\odot}$, the contribution from minor and major mergers are comparable;
- (iii) disc instability represents the dominant contribution to the formation of bulges of intermediate mass galaxies ($\sim 10^{10} - 10^{11} M_{\odot}$).

Qualitatively, our results are in agreement with what

found by Parry et al. (2009), although in their model disc instability plays a more prominent role. It is worrying that such an important contribution to bulge formation comes from the process that we probably model in the poorest way (disc instabilities). The results discussed in this paper confirm that further work is needed in this area in order to improve our galaxy formation models. This is true not just for the criterion adopted to tag a disc as unstable (as discussed for example in Athanassoula 2008), but also for the treatment of these events. In fact, the two models used in this study assume the same mathematical criterion for disc instability but adopt quite different assumptions for the physical quantities considered, and model the outcome of instability events in different ways. In particular, the WDL08 model only transfers to the bulge a fraction of the *stellar* disc that is enough to restore stability. In MORGANA, half of the *baryonic* mass of the disc (i.e. gas and stars) is transferred to the bulge component each time an instability episode occurs. At high redshift, where galaxies are more gas rich and dynamical times are shorter, inflow of gas towards the centre leads to a rapid and efficient growth of the central spheroidal component in this model.

It is instructive to see how different the adopted models are. We can estimate the fraction of discs that are unstable by looking at the distributions of the left-hand side of Eq. 1 for the pure merger models. Results are shown in the bottom panel of Fig. 10, while the other two panels show the distributions of the disc velocity and radius entering Eq. 1 in the same models. The figure shows that there are systematic differences between these quantities in the two models. In particular, the disc velocities and disc scale-lengths used in MORGANA are systematically larger and smaller than those adopted in WDL08, respectively. Despite these differences, the fractions of unstable discs in the two models are comparable: integrating the distributions shown in the bottom panel up to $\epsilon_{\text{lim}} = 0.75$ for WDL08 and $\epsilon_{\text{lim}} = 0.7$ for MORGANA (see Section 2), one obtains that $\sim 5 - 7$ per cent of the discs are unstable in both models. This fraction is approximately independent of redshift. The different treatment of instabilities, however, leads to a much more prominent role of the disc instability channel in MORGANA. To further test our conclusion, we have verified that the contribution from disc instability (particularly at high redshift) is significantly reduced in MORGANA when the fraction of disc mass transferred to the central spheroidal component is reduced from 0.5 to 0.1.

In the framework of our models, bulge dominated galaxies can grow a new disc if they are fed by appreciable cooling flows. The rates of disc regrowth are relatively low at low redshift and for massive galaxies. They are, however, more significant for intermediate and low mass galaxies and at high redshifts, where ellipticals can change back their morphology and become disc dominated galaxies at some later time (i.e. the morphology of these galaxies is *transient*). When an efficient radio-mode feedback is assumed (like in the WDL08 model used here), there is a decline of the typical regrowth rate of the most massive galaxies at low redshift, and of the fraction of these galaxies experiencing regrowth. This is expected given that these galaxies live in the most massive haloes where the radio-mode is assumed to play a major role.

Only a minor fraction of the ellipticals in our models ac-

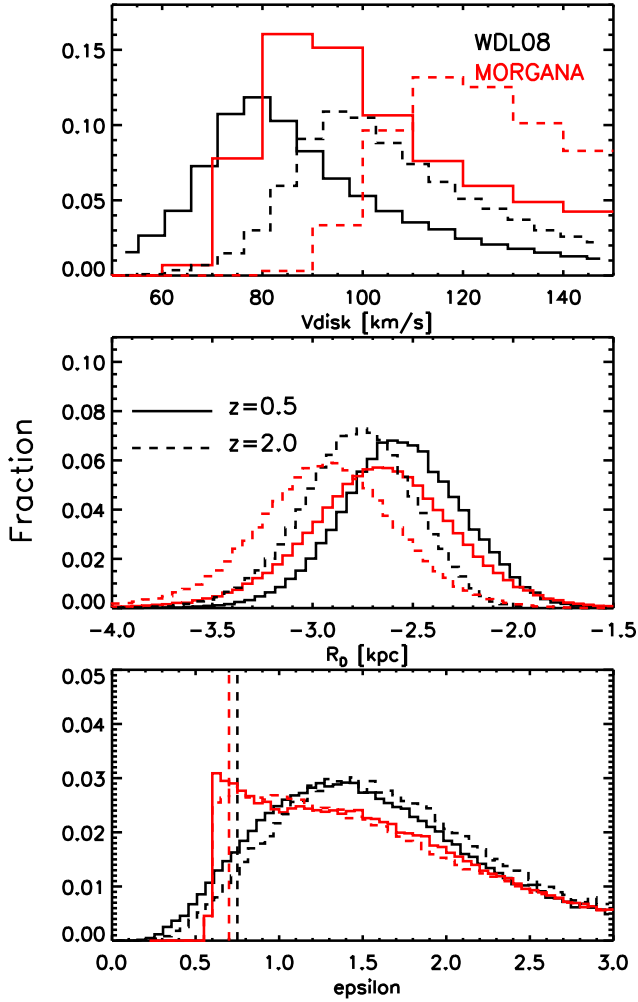


Figure 10. Distributions of the disc velocity and radius entering Eq. 1 at two different redshifts. Black lines correspond to the standard WDL08 model, while red lines are for MORGANA. The bottom panel shows the distribution of the left-hand side of Eq. 1, and the vertical lines mark the threshold for unstable discs adopted in the two models.

quire their morphology through minor mergers. In WDL08, the vast majority of the galaxies become ellipticals through major mergers, and this occurs at relatively low redshift ($z < 2$, only a very small fraction of the galaxies become ellipticals at higher redshift). In MORGANA, the change of morphology occurs at higher redshift, and a large fraction of the galaxies cross the threshold we have adopted to define galaxies as ellipticals ($B/T = 0.9$) as a consequence of disc instabilities. We have demonstrated that this is due to a combination of significantly shorter merger times and a different treatment of disc instability events.

The implementation of a gas-fraction dependent merger model provides trends in bulge-to-total ratio that do not deviate strongly from those of our pure mergers runs at intermediate masses. This appears to be in contradiction with the previous claim of Hopkins et al. (2009) who find that taking into account the gas dependence of merger induced starbursts reduces bulge formation in galaxies less massive

than $\sim 10^{10} M_{\odot}$. We note, however, that the results from the ‘simplified model’ discussed in Hopkins et al. are not representative of the results from our semi-analytic models. In particular, their simplified model provides much more mass in bulges at galaxy masses lower than $\sim 10^{10} M_{\odot}$, where the assumption of a gas dependent merger model should make the largest difference. We note that our standard models do include a dependency on the gas available during minor mergers, and they do so in different ways. The WDL08 model assumes that the stars formed during starbursts associated with these mergers are added to the disc component of the remnant galaxy, while MORGANA adds these stars to the bulge component. The results discussed above show that this model difference does not significantly influence model results, because minor mergers represent a relatively minor contribution to bulge formation.

As explained above, our models naturally predict a strong correlation between the galaxy stellar mass and its morphology. In addition, this correlation evolves in such a way that *fewer* galaxies are bulge dominated at higher redshift. One of the models used in this study (MORGANA) does predict an ‘excess’ of galaxies with large bulge-to-total ratios at intermediate-low masses. As emphasized above, however, this is not due to the fact that the model neglects the dependency on gas fraction. Rather, the behaviour of MORGANA can be ascribed to galaxy merger times that are significantly shorter than those adopted in WDL08, and to a different treatment during instability events that leads to an efficient production of bulges at high redshift. Interestingly, the implementation of a gas-fraction dependent merger model reduces significantly the number of bulge dominated galaxies (ellipticals), and delays their formation. This is a consequence of the assumption that some fraction of the stellar disc is always preserved, even during major mergers.

It remains to be seen if any of the models discussed in this paper provides a good agreement with the growing amount of information being accumulated on the cosmic morphological mix, at different epochs. Such a comparison will certainly represent an important test-bed for the next generation of models, and provide stringent constraints on the mechanisms through which bulges are assembled. While we defer to a forthcoming paper a detailed comparison with observational data, we note that the predicted bulge-to-total distributions (as a function of both stellar and halo mass - see Section 3), as well as the total fraction of bulge-dominated galaxies, are affected by the physical prescriptions adopted to model bulge formation. None of these observables has been used to ‘tune’ the models in the first place, so that they can be considered as genuine model predictions and tested against observational measurements.

We have shown that the contribution to bulge mass from different channels is also affected by the adopted physical modelling. If ‘classical bulges’ are primarily formed through mergers and ‘pseudo-bulges’ can be associated with secular evolution, the results discussed in this paper provide predictions for the relative importance of these two populations, at different cosmic epochs and in different environments. Distinguishing pseudo-bulges from classical bulges is difficult, requires good photometric data and, ideally, also high-resolution spectroscopic information (Debattista et al. 2005). Some statistics are, however, available at low redshift (Gadotti 2009) and can be used to constrain our models.

ACKNOWLEDGEMENTS

We are grateful to Jie Wang for letting us use the outputs of his simulations. GDL acknowledges financial support from the European Research Council under the European Community's Seventh Framework Programme (FP7/2007-2013)/ERC grant agreement n. 202781. FF acknowledges the support of an INAF-OATs fellowship granted on 'Basic Research' funds. DW acknowledges the support of the Max-Planck Gesellschaft.

This paper has been typeset from a \LaTeX file prepared by the author.

REFERENCES

- Andredakis Y. C., Sanders R. H., 1994, *MNRAS*, 267, 283
 Athanassoula E., 2008, *MNRAS*, 390, L69
 Balcells M., Graham A. W., Domínguez-Palmero L., Peletier R. F., 2003, *ApJ*, 582, L79
 Benson A. J., Devereux N., 2010, *MNRAS*, 402, 2321
 Bower R. G., Benson A. J., Malbon R., Helly J. C., Frenk C. S., Baugh C. M., Cole S., Lacey C. G., 2006, *MNRAS*, 370, 645
 Carollo C. M., Stiavelli M., de Zeeuw P. T., Seigar M., Dejonghe H., 2001, *ApJ*, 546, 216
 Combes F., Debbasch F., Friedli D., Pfenniger D., 1990, *A&A*, 233, 82
 Cox T. J., Jonsson P., Somerville R. S., Primack J. R., Dekel A., 2008, *MNRAS*, 384, 386
 Davies R. L., Illingworth G., 1983, *ApJ*, 266, 516
 De Lucia G., Blaizot J., 2007, *MNRAS*, 375, 2
 De Lucia G., Boylan-Kolchin M., Benson A. J., Fontanot F., Monaco P., 2010, *MNRAS*, 406, 1533
 De Lucia G., Helmi A., 2008, *MNRAS*, 391, 14
 De Lucia G., Kauffmann G., Springel V., White S. D. M., Lanzoni B., Stoehr F., Tormen G., Yoshida N., 2004, *MNRAS*, 348, 333
 De Lucia G., Springel V., White S. D. M., Croton D., Kauffmann G., 2006, *MNRAS*, 366, 499
 Debattista V. P., Carollo C. M., Mayer L., Moore B., 2005, *ApJ*, 628, 678
 Debattista V. P., Mayer L., Carollo C. M., Moore B., Wadsley J., Quinn T., 2006, *ApJ*, 645, 209
 Dressler A., Sandage A., 1983, *ApJ*, 265, 664
 Efstathiou G., Lake G., Negroponte J., 1982, *MNRAS*, 199, 1069
 Fisher D. B., Drory N., 2008, *AJ*, 136, 773
 Fontanot F., De Lucia G., Monaco P., Somerville R. S., Santini P., 2009, *MNRAS*, 397, 1776
 Fontanot F., Pasquali A., De Lucia G., van den Bosch F. C., Somerville R. S., Kang X., 2010, *ArXiv:1006.5717*
 Gadotti D. A., 2009, *MNRAS*, 393, 1531
 Gao L., White S. D. M., Jenkins A., Stoehr F., Springel V., 2004, *MNRAS*, 355, 819
 Hohl F., 1971, *ApJ*, 168, 343
 Hopkins P. F., Cox T. J., Younger J. D., Hernquist L., 2009, *ApJ*, 691, 1168
 Hopkins P. F., Somerville R. S., Cox T. J., Hernquist L., Jogee S., Kereš D., Ma C., Robertson B., Stewart K., 2009, *MNRAS*, 397, 802
 Hubble E. P., 1926, *ApJ*, 64, 321
 Kimm T., Somerville R. S., Yi S. K., van den Bosch F. C., Salim S., Fontanot F., Monaco P., Mo H., Pasquali A., Rich R. M., Yang X., 2009, *MNRAS*, 394, 1131
 Kormendy J., 1993, in H. Dejonghe & H. J. Habing ed., *Galactic Bulges Vol. 153 of IAU Symposium, Kinematics of extragalactic bulges: evidence that some bulges are really disks.* p. 209
 Kormendy J., Illingworth G., 1982, *ApJ*, 256, 460
 Kormendy J., Kennicutt Jr. R. C., 2004, *ARA&A*, 42, 603
 Li Y., De Lucia G., Helmi A., 2010, *MNRAS*, 401, 2036
 Li Y., Mo H. J., van den Bosch F. C., Lin W. P., 2007, *MNRAS*, 379, 689
 Lo Faro B., Monaco P., Vanzella E., Fontanot F., Silva L., Cristiani S., 2009, *MNRAS*, 399, 827
 Macciò A. V., Kang X., Fontanot F., Somerville R. S., Kopeck S., Monaco P., 2010, *MNRAS*, 402, 1995
 Mihos J. C., 2004, *Clusters of Galaxies: Probes of Cosmological Structure and Galaxy Evolution*, p. 277
 Mo H. J., Mao S., White S. D. M., 1998, *MNRAS*, 295, 319
 Monaco P., Fontanot F., Taffoni G., 2007, *MNRAS*, 375, 1189
 Monaco P., Theuns T., Taffoni G., Governato F., Quinn T., Stadel J., 2002, *ApJ*, 564, 8
 Parry O. H., Eke V. R., Frenk C. S., 2009, *MNRAS*, 396, 1972
 Pinkney J., Gebhardt K., Bender R., Bower G., Dressler A., Faber S. M., Filippenko A. V., Green R., Ho L. C., Kormendy J., Lauer T. R., Magorrian J., Richstone D., Tremaine S., 2003, *ApJ*, 596, 903
 Raha N., Sellwood J. A., James R. A., Kahn F. D., 1991, *Nature*, 352, 411
 Somerville R. S., Hopkins P. F., Cox T. J., Robertson B. E., Hernquist L., 2008, *MNRAS*, 391, 481
 Somerville R. S., Primack J. R., Faber S. M., 2001, *MNRAS*, 320, 504
 Springel V., Di Matteo T., Hernquist L., 2005, *MNRAS*, 361, 776
 Springel V., White S. D. M., Jenkins A., Frenk C. S., Yoshida N., Gao L., Navarro J., Thacker R., Croton D., Helly J., Peacock J. A., Cole S., Thomas P., Couchman H., Evrard A., Colberg J., Pearce F., 2005, *Nature*, 435, 629
 Springel V., White S. D. M., Tormen G., Kauffmann G., 2001, *MNRAS*, 328, 726
 Taffoni G., Mayer L., Colpi M., Governato F., 2003, *MNRAS*, 341, 434
 Taffoni G., Monaco P., Theuns T., 2002, *MNRAS*, 333, 623
 Toomre A., Toomre J., 1972, *ApJ*, 178, 623
 Wang J., De Lucia G., Kitzbichler M. G., White S. D. M., 2008, *MNRAS*, 384, 1301
 Weinmann S. M., Kauffmann G., von der Linden A., De Lucia G., 2010, *MNRAS*, 406, 2249
 Wilman D. J., Oemler A., Mulchaey J. S., McGee S. L., Balogh M. L., Bower R. G., 2009, *ApJ*, 692, 298